The Heteronuclear Cluster Chemistry of the Group 1B Metals. Part 6.[1] Synthesis, Structures, and Dynamic Behaviour of the Bimetallic Hexanuclear Group 1B Metal Cluster Compounds $[M_2Ru_4(\mu_3\text{-}H)_2\{\mu\text{-}Ph_2P(CH_2)_nPPh_2\}(CO)_{12}]$ (M = Cu or Ag, *n* = 1—6). *X*-Ray Crystal Structures of $[Cu_2Ru_4(\mu_3\text{-}H)_2\{\mu\text{-}Ph_2P(CH_2)_nPPh_2\}(CO)_{12}]$ (*n* = 2, 3, or 5)†

Scott S. D. Brown and Ian D. Salter *
Department of Chemistry, University of Exeter, Exeter EX4 4QD
Loïc Toupet
Laboratoire de Physique Cristalline, Department de Physique, U.A. 04804, Campus de Beaulieu, Universite de Rennes, 35042 Rennes-Cedex, France

---

Treatment of a dichloromethane solution of the salt $[N(PPh_3)_2]_2[Ru_4(\mu\text{-}H)_2(CO)_{12}]$ with two equivalents of the complex $[M(NCMe)_4]PF_6$ (M = Cu or Ag) at −30 °C, followed by the addition of one equivalent of $Ph_2P(CH_2)_nPPh_2$ (*n* = 1—6) affords the mixed-metal cluster compounds $[M_2Ru_4(\mu_3\text{-}H)_2\{\mu\text{-}Ph_2P(CH_2)_nPPh_2\}(CO)_{12}]$ in *ca.* 65—75% yield. These species have been characterized by i.r. and n.m.r. spectroscopy and the structures of $[Cu_2Ru_4(\mu_3\text{-}H)_2\{\mu\text{-}Ph_2P(CH_2)_nPPh_2\}(CO)_{12}]$ (*n* = 2, 3, or 5) have been determined by *X*-ray diffraction studies. The clusters all adopt the same metal core structure, which consists of a tetrahedron of ruthenium atoms capped by a Group 1B metal, with one of the MRu_2 faces of the MRu_3 tetrahedron so formed further capped by a second Group 1B metal to give a capped trigonal-bipyramidal skeletal geometry. The other two MRu_2 faces of the MRu_3 tetrahedron are each capped by a triply-bridging hydrido ligand, the bidentate diphosphine ligand bridges the two coinage metals, and each ruthenium atom is ligated by three terminal CO groups. Variable-temperature ^1H and $^{31}P\text{-}\{^1H\}$ n.m.r. studies show that, at ambient temperature in solution, the metal frameworks of all of the clusters still undergo dynamic behaviour involving coinage metal site-exchange, even though the two Group 1B metals are linked together by bidentate diphosphine ligands.

An interesting feature of the chemistry of Group 1B metal heteronuclear cluster compounds is the stereochemical non-rigidity exhibited in solution by the metal skeletons of some species which contain two or more $M(PR_3)$ (M = Cu, Ag, or Au; R = alkyl or aryl) units.[1—3] Dynamic behaviour which is thought to involve coinage metal site-exchange is frequently observed when $M(PR_3)$ moieties adopt structurally inequivalent positions in the ground-state geometries of such clusters.[1—3] For example, single-crystal *X*-ray diffraction studies reveal that, in the solid state, the clusters $[M_2Ru_4(\mu_3\text{-}H)_2(CO)_{12}(PPh_3)_2]$ [M = Cu (**1**) or Ag (**2**)] exhibit capped trigonal-bipyramidal metal frameworks, with two geometrically distinct $M(PPh_3)$ sites.[3] However, single resonances were observed in the $^{31}P\text{-}\{^1H\}$ n.m.r. spectra of (**1**) and (**2**) at ambient temperature and −50 °C, respectively, although spectra consistent with the ground-state structures were obtained at −90 °C.[3] An intramolecular rearrangement of the metal skeletons of the clusters in solution was proposed[3] to explain the results.

Although a large number of examples of heteronuclear clusters containing one or more Group 1B metals ligated by monodentate phosphine groups have now been reported,[4] detailed studies of similar species containing bidentate diphosphine ligands are still relatively rare.[1,5—10] Therefore, we wished to synthesize a series of clusters analogous to (**1**) and (**2**), in which the two coinage metals are linked by the bidentate diphosphine ligands $Ph_2P(CH_2)_nPPh_2$ (*n* = 1—6), and to investigate whether the structures and dynamic behaviour of these species are similar to those exhibited by (**1**) and (**2**). Herein we report the synthesis, structural characterization, and variable-temperature ^1H and $^{31}P\text{-}\{^1H\}$ n.m.r. spectra of the mixed-metal clusters $[M_2Ru_4(\mu_3\text{-}H)_2\{\mu\text{-}Ph_2P(CH_2)_nPPh_2\}(CO)_{12}]$ (M = Cu or Ag; *n* = 1—6). A preliminary account describing some of our results has already been published.[11]

Results and Discussion

Treatment of a dichloromethane solution of the salt $[N(PPh_3)_2]_2[Ru_4(\mu\text{-}H)_2(CO)_{12}]$ with two equivalents of the complex $[M(NCMe)_4]PF_6$ (M = Cu or Ag) at −30 °C incorporates two M(NCMe) units into the cluster dianion and subsequent addition of one equivalent of the appropriate bidentate diphosphine $Ph_2P(CH_2)_nPPh_2$ (*n* = 1—6) affords the dark red cluster compounds $[M_2Ru_4(\mu_3\text{-}H)_2\{\mu\text{-}Ph_2P(CH_2)_nPPh_2\}(CO)_{12}]$ [M = Cu, *n* = 1 (**3**), 2 (**4**), 3 (**5**), 4 (**6**), 5 (**7**), or 6 (**8**); M = Ag, *n* = 1 (**9**), 2 (**10**), 3 (**11**), 4 (**12**), 5 (**13**), 6 (**14**)] in *ca.* 65—75% yield. The clusters (**3**)—(**14**) were characterized by microanalysis and by spectroscopic measurements (Tables 1 and 2). The i.r. spectra of (**3**)—(**14**) are almost identical and they are closely similar to those of (**1**) and (**2**),[3] implying that all these species adopt the same capped trigonal-bipyramidal metal core geometry. The n.m.r. spectroscopic data and microanalyses are fully consistent with the proposed formulations for (**3**)—(**14**), but to investigate the detailed structures of some representative examples of this series of clusters, single-crystal *X*-ray diffraction studies were performed on (**4**), (**5**), and (**7**). Discussion of the variable-temperature n.m.r.

---

† 1,2-μ-[1′,2′-bis(diphenylphosphino)ethane]-, 1,2-μ-[1′,3′-bis(diphenylphosphino)propane]-, and 1,2-μ-[1′,5′-bis(diphenylphosphino)pentane]-3,3,3,4,4,4,5,5,5,6,6,6-dodecacarbonyl-1,3,5;1,4,5-di-μ-hydrido-*cyclo*-1,2-dicopper-3,4,5,6-tetraruthenium (*Cu–Cu*) (5 *Cu–Ru*) (6 *Ru–Ru*).

Supplementary data available: see Instructions for Authors, *J. Chem. Soc., Dalton Trans.*, 1988, Issue 1, pp. xvii–xx.

Table 1. Analytical[a] and physical data for the new Group 1B metal heteronuclear cluster compounds

Compound	M.p. (θ_c/°C) (decomp.)	$\nu_{max.}$(CO)[b]/cm^{-1}	Yield (%)[c]	Analysis (%)[d]	
				C	H
(**3**) $[Cu_2Ru_4(\mu_3\text{-}H)_2(\mu\text{-}Ph_2PCH_2PPh_2)(CO)_{12}]$	143—147	2 071s, 2 036vs, 2 021vs, 2 009s, 1 979w br, 1 934w br	68	35.7 (35.4)	1.9 (1.9)
(**4**) $[Cu_2Ru_4(\mu_3\text{-}H)_2\{\mu\text{-}Ph_2P(CH_2)_2PPh_2\}(CO)_{12}]$	167—170	2 071s, 2 034vs, 2 021vs, 2 006s, 1 979w br, 1 936w br	72	36.1 (36.0)	2.2 (2.1)
(**5**) $[Cu_2Ru_4(\mu_3\text{-}H)_2\{\mu\text{-}Ph_2P(CH_2)_3PPh_2\}(CO)_{12}]$	167—171	2 071s, 2 034vs, 2 021vs, 2 007s, 1 977w br, 1 935w br	69	36.3 (36.5)	2.2 (2.2)
(**6**) $[Cu_2Ru_4(\mu_3\text{-}H)_2\{\mu\text{-}Ph_2P(CH_2)_4PPh_2\}(CO)_{12}]$	174—178	2 071s, 2 034vs, 2 021vs, 2 006s, 1 979w br, 1 934w br	75	36.9 (37.1)	2.3 (2.3)
(**7**) $[Cu_2Ru_4(\mu_3\text{-}H)_2\{\mu\text{-}Ph_2P(CH_2)_5PPh_2\}(CO)_{12}]$	169—172	2 071s, 2 034vs, 2 021vs, 2 006s, 1 979w br, 1 931w br	68	37.4 (37.6)	2.5 (2.5)
(**8**) $[Cu_2Ru_4(\mu_3\text{-}H)_2\{\mu\text{-}Ph_2P(CH_2)_6PPh_2\}(CO)_{12}]$	155—158	2 072s, 2 033vs, 2 021vs, 2 007s, 1 976w br, 1 932w br	65	38.1 (38.1)	2.9 (2.6)
(**9**) $[Ag_2Ru_4(\mu_3\text{-}H)_2(\mu\text{-}Ph_2PCH_2PPh_2)(CO)_{12}]$	164—168	2 065s, 2 029vs, 2 013vs, 2 003 (sh), 1 967m br, 1 925w br	74	33.3 (33.1)	2.0 (1.8)
(**10**) $[Ag_2Ru_4(\mu_3\text{-}H)_2\{\mu\text{-}Ph_2P(CH_2)_2PPh_2\}(CO)_{12}]$	218—222	2 067s, 2 029vs, 2 016vs, 2 000s, 1 969m br, 1 927w br	72	33.4 (33.6)	1.6 (1.9)
(**11**) $[Ag_2Ru_4(\mu_3\text{-}H)_2\{\mu\text{-}Ph_2P(CH_2)_3PPh_2\}(CO)_{12}]$	127—134	2 066s, 2 028vs, 2 015vs, 2 000s, 1 968m br, 1 928w br	65	33.7 (34.2)	1.9 (2.0)
(**12**) $[Ag_2Ru_4(\mu_3\text{-}H)_2\{\mu\text{-}Ph_2P(CH_2)_4PPh_2\}(CO)_{12}]$	138—140	2 066s, 2 028vs, 2 016vs, 2 000s, 1 967m br, 1 927w br	69	34.6 (34.7)	2.5 (2.2)
(**13**) $[Ag_2Ru_4(\mu_3\text{-}H)_2\{\mu\text{-}Ph_2P(CH_2)_5PPh_2\}(CO)_{12}]$	141—144	2 070s, 2 032vs, 2 019vs, 2 003s, 1 974m br, 1 933w br	76	35.0 (35.2)	2.2 (2.3)
(**14**) $[Ag_2Ru_4(\mu_3\text{-}H)_2\{\mu\text{-}Ph_2P(CH_2)_6PPh_2\}(CO)_{12}]$	148—150	2 071s, 2 032vs, 2 020vs, 2 004s, 1 973m br, 1 935w br	70	35.7 (35.7)	2.4 (2.4)

[a] Calculated values given in parentheses. [b] Measured in dichloromethane solution. [c] Based on ruthenium reactant. [d] Although large crystals of (**4**), (**5**), and (**7**), grown slowly over a period of days so that they were suitable for *X*-ray diffraction studies are dichloromethane solvates, when *microcrystals* of these clusters were grown quickly for analysis, no evidence of dichloromethane of crystallization was found.

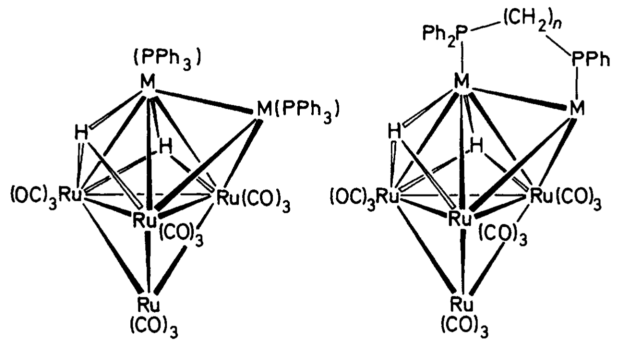

M = Cu (**1**) or Ag (**2**)

M = Cu; n = 1 (**3**), 2 (**4**), 3 (**5**), 4 (**6**), 5 (**7**), 6 (**8**)
M = Ag; n = 1 (**9**), 2 (**10**), 3 (**11**), 4 (**12**), 5 (**13**), 6 (**14**)

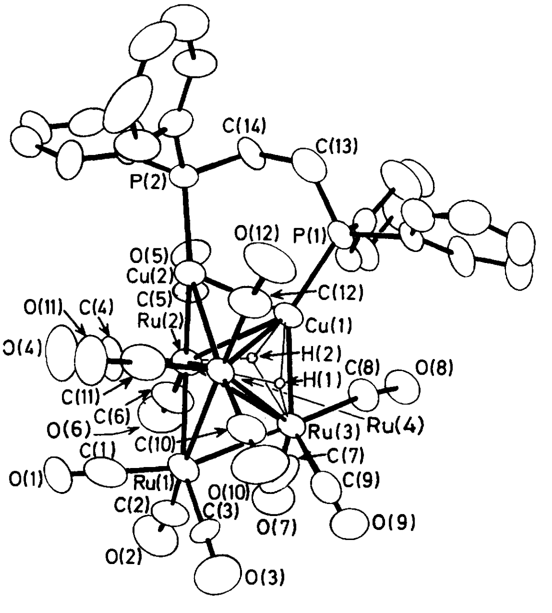

Figure 1. Molecular structure of $[Cu_2Ru_4(\mu_3\text{-}H)_2\{\mu\text{-}Ph_2P(CH_2)_2\text{-}PPh_2\}(CO)_{12}]$ (**4**), showing the crystallographic numbering

data is best deferred until the *X*-ray diffraction results have been described.

The molecular structures of (**4**), (**5**), and (**7**) are illustrated in Figures 1, 2, and 3, respectively, which also show the crystallographic numbering. Compound (**4**) crystallizes with two independent molecules (A and B) in the asymmetric unit and some of the parameters for A and B are significantly different. Therefore, selected interatomic distances and angles for both molecules of (**4**), together with values for (**5**) and (**7**), are summarized in Tables 3 and 4.

The metal skeletons of (**4**), (**5**), and (**7**) adopt the same capped trigonal-bipyramidal structure as that established for the analogous PPh_3-containing cluster (**1**). The four Ru atoms form a tetrahedron, with one face [Ru(2)Ru(3)Ru(4)] capped by a copper atom [Cu(1)] and the Cu(1)Ru(2)Ru(4) face of the $CuRu_3$ tetrahedron so formed further capped by a second copper atom [Cu(2)]. In each cluster, the bidentate diphosphine ligand bridges the Cu–Cu vector, both the Cu(1)Ru(2)Ru(3) and the Cu(1)Ru(3)Ru(4) faces of the metal skeleton are capped by a triply bridging hydrido ligand and the Ru atoms are all ligated by three terminal CO groups, which are essentially linear.

Figure 4 compares the values of the metal–metal separations in the frameworks of (**4**), (**5**), and (**7**) with those of (**1**). As expected,[3] the lengths of the three unbridged Ru–Ru vectors

Table 2. Hydrogen-1 and phosphorus-31 n.m.r. data[a] for the new Group 1B metal cluster compounds

Complex	Ambient-temperature ^{1}H data[b]	Low-temperature ^{1}H hydrido ligand signal[b,c]	Ambient-temperature ^{31}P-{^{1}H} data[d]	Low-temperautre ^{31}P-{^{1}H} data[c,d]
(**3**)	−18.01 [t, 2 H, μ_3-H, *J*(PH) 7], 3.51 [t, 2 H, $\mathrm{PCH_2P}$, *J*(PH) 11], 7.37—7.54 (m, 20 H, Ph)	[e] −18.17 [d, 2 H, *J*(PH) 13]	−3.2 (s, br)	2.9 [d, *J*(PP) 91], −8.9 [d, *J*(PP) 91]
(**4**)	−17.67 [t, 2 H, μ_3-H, *J*(PH) 6], 2.61—2.71 (m, 4 H, $\mathrm{PCH_2CH_2P}$), 7.47—7.71 (m, 20 H, Ph)	[e] −17.84 [d, 1 H, *J*(PH) 13], −17.63 [d, 1 H, *J*(PH) 12]	−0.4 (s, br)	[f] 3.7 (s), −4.5 (s)
(**5**)	−17.56 [t, 2 H, μ_3-H, *J*(PH) 6], 2.03—2.16 (m, 2 H, $\mathrm{PCH_2C}\mathit{H}_2\mathrm{CH_2P}$), 2.62—2.68 (m, 4 H, $\mathrm{PC}\mathit{H}_2\mathrm{CH_2C}\mathit{H}_2\mathrm{P}$), 7.44—7.58 (m, 20 H, Ph)	[g] −17.69 [d, 2 H, *J*(PH) 13]	1.0 (s, br)	[g] 5.9 (s), −3.9 (s)
(**6**)	−17.37 [t, 2 H, μ_3-H, *J*(PH) 6], 1.88 (s, vbr, 4 H, $\mathrm{PCH_2C}\mathit{H}_2\mathrm{C}\mathit{H}_2\mathrm{CH_2P}$), 2.58—2.64 (m, 4 H, $\mathrm{PC}\mathit{H}_2\mathrm{CH_2CH_2C}\mathit{H}_2\mathrm{P}$), 7.48—7.60 (m, 20 H, Ph)	[g] −17.50 [d, 2 H, *J*(PH) 12]	−3.9 (s, br)	6.8 (s), −14.5 (s)
(**7**)	−17.20 [t, 2 H, μ_3-H, *J*(PH) 6], 1.38—1.77 (m, 6 H, $\mathrm{PCH_2C}\mathit{H}_2\mathrm{C}\mathit{H}_2\mathrm{C}\mathit{H}_2\mathrm{CH_2P}$), 2.27—2.50 (m, 4 H, $\mathrm{PC}\mathit{H}_2\mathrm{CH_2CH_2CH_2C}\mathit{H}_2\mathrm{P}$), 7.04—7.67 (m, 20 H, Ph)	−17.31 [d, 2 H, *J*(PH) 12]	−2.8 (s, br)	[g] 5.4 (s), −11.1 (s)
(**8**)	−16.79 [t, 2 H, μ_3-H, *J*(PH) 6], 1.62 (s, vbr, 8 H, $\mathrm{PCH_2C}\mathit{H}_2\mathrm{C}\mathit{H}_2\mathrm{C}\mathit{H}_2\mathrm{C}\mathit{H}_2\mathrm{CH_2P}$), 2.28—2.32 (m, 4 H, $\mathrm{PC}\mathit{H}_2\mathrm{CH_2CH_2CH_2CH_2C}\mathit{H}_2\mathrm{P}$), 7.27—7.64 (m, 20 H, Ph)	[h] −17.02 [d, 2 H, *J*(PH) 12]	1.0 (s, br)	5.0 (s), −1.6 (s)
(**9**)	−17.72 [apparent t of t of t, 2 H, μ_3-H, *J*(^{109}AgH) 20, *J*(^{107}AgH) 17, *J*(PH) 5], 3.52 [t of t, 2 H, $\mathrm{PCH_2P}$, *J*(PH) 10, *J*(AgH)$_{\mathrm{av}}$ 4], 7.14—7.55 (m, 20 H, Ph)	[e] −17.93 [apparent t of t, 2 H, *J*(AgH)$_{\mathrm{av}}$ 18, *J*(PH) 5]	6.7 (m)	[e] *ca.* 6 (s, vbr)
(**10**)	−17.47 [apparent t of t of t, 2 H, μ_3-H, *J*(^{109}AgH) 18, *J*(^{107}AgH) 16, *J*(PH) 5], 2.48—2.59 (m, 4 H, $\mathrm{PCH_2CH_2P}$), 7.50—7.64 (m, 20 H, Ph)	[e] −17.59 [d, br, 2 H, *J*(AgH)$_{\mathrm{av}}$ 30]	12.9 (m)	[e] 15.0 [2 × d, br, *J*(^{109}AgP) 586, *J*(^{107}AgP) 509], 11.2 [2 × d, br, *J*(^{109}AgP) 456, *J*(^{107}AgP) 395]
(**11**)	−17.42 [apparent t of t of t, 2 H, μ_3-H, *J*(^{109}AgH) 17, *J*(^{107}AgH) 15, *J*(PH) 5], 2.04—2.22 (m, 2 H, $\mathrm{PCH_2C}\mathit{H}_2\mathrm{CH_2P}$), 2.53—2.56 (m, 4 H, $\mathrm{PC}\mathit{H}_2\mathrm{CH_2C}\mathit{H}_2\mathrm{P}$), 7.47—7.53 (m, 20 H, Ph)	−17.54 [d of d, 2 H, *J*(AgH)$_{\mathrm{av}}$ 33, *J*(PH) 9]	15.8 (m)	[i] 18.7 [2 × d of d, *J*(^{109}AgP) 590, *J*(^{107}AgP) 509, ^{2}*J*(AgP)$_{\mathrm{av}}$ 7], 14.3 [2 × d of d, *J*(^{109}AgP) 471, *J*(^{107}AgP) 405, ^{2}*J*(AgP)$_{\mathrm{av}}$ 6]
(**12**)	−17.26 [apparent t of t of t, 2 H, μ_3-H, *J*(^{109}AgH) 17, *J*(^{107}AgH) 15, *J*(PH) 5], 1.96—2.02 (m, 4 H, $\mathrm{PCH_2C}\mathit{H}_2\mathrm{C}\mathit{H}_2\mathrm{CH_2P}$), 2.49—2.53 (m, 4 H, $\mathrm{PC}\mathit{H}_2\mathrm{CH_2CH_2C}\mathit{H}_2\mathrm{P}$), 7.49—7.62 (m, 20 H, Ph)	−17.39 [d of d, 2 H, *J*(AgH)$_{\mathrm{av}}$ 31, *J*(PH) 10]	9.5 (*m*)	18.4 [2 × d of d, *J*(^{109}AgP) 583, *J*(^{107}AgP) 505, ^{2}*J*(AgP)$_{\mathrm{av}}$ 4], −1.3 [2 × d of d, *J*(^{109}AgP) 479,*J*(^{107}AgP)415,^{2}*J*(AgP)$_{\mathrm{av}}$11]
(**13**)	−17.10 [apparent t of t of t, 2 H, μ_3-H, *J*(^{109}AgH) 15, *J*(^{107}AgH) 13, *J*(PH) 5], 1.59—1.71 (m, 4 H, $\mathrm{PCH_2C}\mathit{H}_2\mathrm{CH_2C}\mathit{H}_2\mathrm{CH_2P}$), 2.02—2.08 (m, 2 H, $\mathrm{PCH_2CH_2C}\mathit{H}_2\mathrm{CH_2CH_2P}$), 2.45—2.58 (m, 4 H, $\mathrm{PC}\mathit{H}_2\mathrm{CH_2CH_2CH_2C}\mathit{H}_2\mathrm{P}$), 7.58—7.73 (m, 20 H, Ph)	−17.18 [d of d, 2 H, *J*(AgH)$_{\mathrm{av}}$ 26, *J*(PH) 9]	6.4 (m)	7.4 [2 × d of d, *J*(^{109}AgP) 573, *J*(^{107}AgP) 497, ^{2}*J*(AgP)$_{\mathrm{av}}$ 7], −0.2 [2 × d of d, *J*(^{109}AgP) 488,*J*(^{107}AgP)423,^{2}*J*(AgP)$_{\mathrm{av}}$11]
(**14**)	−17.00 [apparent t of t of t, 2 H, μ_3-H, *J*(^{109}AgH) 14, *J*(^{107}AgH) 12, *J*(PH) 5], 1.56—1.63 (m, 4 H, $\mathrm{PCH_2CH_2C}\mathit{H}_2\mathrm{C}\mathit{H}_2\mathrm{CH_2CH_2P}$), 1.65—1.76 (m, 4 H, $\mathrm{PCH_2C}\mathit{H}_2\mathrm{CH_2CH_2C}\mathit{H}_2\mathrm{CH_2P}$), 2.28—2.35 (m, 4 H, $\mathrm{PC}\mathit{H}_2\mathrm{CH_2CH_2CH_2CH_2C}\mathit{H}_2\mathrm{P}$), 7.47—7.60 (m, 20 H, Ph)	−17.11 [d of d, 2 H, *J*(AgH)$_{\mathrm{av}}$ 25, *J*(PH) 9]	14.0 (m)	16.8 [2 × d of d, *J*(^{109}AgP) 570, *J*(^{107}AgP) 509, ^{2}*J*(AgP)$_{\mathrm{av}}$ 8], 12.2 [2 × d of d, *J*(^{109}AgP) 487, *J*(^{107}AgP) 423, ^{2}*J*(AgP)$_{\mathrm{av}}$ 12]

[a] Chemical shifts (δ) in p.p.m., coupling constants in Hz. [b] Measured in [$^2H_2$]dichloromethane solution. [c] Measured at −90 °C, unless otherwise stated. [d] Hydrogen-1 decoupled, measured in [$^2H_2$]dichloromethane–CH_2Cl_2 solution, chemical shifts positive to high frequency of 85% H_3PO_4 (external). [e] Measured at −100 °C. [f] Measured at −65 °C. [g] Measured at −60 °C. [h] Measured at −80 °C. [i] Measured at −95 °C.

[Ru(1)–Ru(2), Ru(1)–Ru(3), and Ru(1)–Ru(4)] in the Ru_4 tetrahedra of (**1**), (**4**), (**5**), and (**7**) are altered very little by the changes in phosphine ligand, but most of the other metal–metal separations vary significantly. The Cu–Cu distance in (**5**) [2.568(1) Å] is *ca.* 0.07 Å larger than the corresponding separation in (**4**) [mean value 2.499(3) Å] and the addition of two more CH_2 groups to the diphosphine backbone in (**7**) further lengthens this vector by *ca.* 0.09 Å [2.659(1) Å]. Replacement of the $Ph_2P(CH_2)_5PPh_2$ ligand in (**7**) by two PPh_3 groups in (**1**) causes a further increase of *ca.* 0.04 Å in the Cu–Cu separation [2.699(2) Å]. The Cu(1)–Ru(3) separations in (**4**), (**5**), and (**7**) are all significantly shorter than the corresponding distance in (**1**) [2.809(2) Å] and they lengthen steadily as the number of CH_2 groups in the diphosphine backbone increases. The distance in (**4**) [mean value 2.676(3) Å] is *ca.* 0.07 Å shorter than that in (**5**) [2.742(1) Å] and *ca.* 0.11 Å shorter than that in (**7**) [2.782(1) Å]. The Cu(2)–Ru(2) and Cu(2)–Ru(4) distances in (**4**), (**5**), and (**7**) are all significantly shorter than the corresponding separations in (**1**), whereas the Cu(1)–Ru(2) and Cu(1)–Ru(4) vectors in these species are all longer than the equivalent values in (**1**). The nature of the attached phosphine ligand has a much smaller effect on the lengths of the Ru–Ru vectors capped by $Cu(PR_3)$ moieties or hydrido ligands [Ru(2)–Ru(3), Ru(2)–Ru(4), and Ru(3)–Ru(4)] in (**1**), (**4**), (**5**), and (**7**), with the variations lying in the range *ca.* 0.02—0.04 Å.

The Cu–P separations in (**4**), (**5**), and (**7**) range from 2.176(7) to 2.238(7) Å, similar to values previously observed in cluster compounds containing $Cu(PR_3)$ fragments.[5,12] The metal–carbonyl angles for all three clusters are very similar [M–C–O 168(2)—180(1)° for (**4**), 171.5(7)—177.9(9)° for (**5**), and 169.4(9)—178.4(8)° for (**7**)] and they all lie in the range normally observed for terminal CO ligands. Unusually short Cu–C contacts between copper atoms and essentially linear CO ligands bonded to adjacent metals have been observed previously in a number of heteronuclear cluster compounds containing CuL (L = two-electron donor ligand)/moieties[5,12–14] and some CO groups in (**4**), (**5**), and (**7**) exhibit similar behaviour. The separations Cu(1)–C(12), Cu(2)–C(12), Cu(2)–C(5), and Cu(2)–C(11) in (**4**), (**5**), and (**7**), together with Cu(1)–C(8) in (**4**) and (**5**) and Cu(2)–C(4) in (**5**) and (**7**), all lie in the range 2.56(2)–2.92(2) Å.

Having established the molecular structures of (**4**), (**5**), and (**7**), it is possible to interpret the variable-temperature n.m.r. spectra of (**3**)—(**14**) (Table 2). The variable-temperature n.m.r. spectra of the copper clusters (**3**)—(**8**) are very similar to those reported[3] for the analogous PPh_3 species (**1**). At ambient temperature, the ^{31}P-{^{1}H} n.m.r. spectrum for each of (**3**)—(**8**) consists of a singlet broadened by quadrupolar effects from the copper atoms.[3,5,12,15] However, at low temperature, two phosphorus resonances are observed, consistent with the ground-state structures of the clusters. The high-field hydrido ligand signals in the ambient-temperature ^{1}H n.m.r. spectra of (**3**)—(**8**) are triplets [*J*(PH) 6—7 Hz], showing coupling to two equivalent phosphorus atoms. However, at low temperature, the ^{1}H n.m.r. hydrido ligand peaks are doublets [*J*(PH) 12—13 Hz] and these signals are consistent with the ground-state geometries, in which the phosphorus atom at P(1) would be expected to show coupling to the hydrido ligands, but that at P(2) would not.[3]

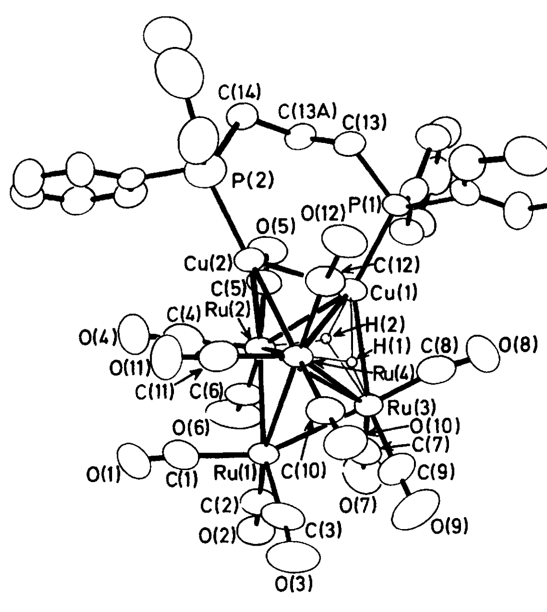

Figure 2. Molecular structure of $[Cu_2Ru_4(\mu_3\text{-}H)_2\{\mu\text{-}Ph_2P(CH_2)_3\text{-}PPh_2\}(CO)_{12}]$ (**5**), showing the crystallographic numbering

In contrast to the ambient-temperature ^{31}P-{^{1}H} n.m.r. spectrum of the silver cluster (**2**), which is severely broadened by dynamic behaviour involving an intermolecular exchange of PPh_3 groups, the spectra of (**9**)—(**14**) consist of complex multiplets, with narrow linewidths. Analysis[16] of these multiplets demonstrates that each cluster exhibits a single averaged phosphorus environment and that the complexity of the signals is caused by a combination of second-order effects, ^{107,109}Ag–^{31}P couplings through one and two bonds, ^{107,109}Ag–^{107,109}Ag couplings and, in some cases, ^{31}P–^{31}P couplings. The observation of ^{107,109}Ag–^{31}P couplings demonstrates that the $Ph_2P(CH_2)_nPPh_2$ (n = 1—6) ligands in (**9**)—(**14**) do not exchange between clusters at ambient temperatures in solution. The ^{31}P-{^{1}H} n.m.r. spectrum of (**9**) at −100 °C is very severely broadened, but two phosphorus resonances, consistent with the ground-state structures of the clusters, are visible in the low-temperature spectra of (**10**)—(**14**). The resonance for each environment is split into two doublets by the large ^{109}Ag–^{31}P and ^{107}Ag–^{31}P couplings through one bond and, in the case of (**11**)—(**14**), these doublets are all further split by an extra, small ^{107,109}Ag–^{31}P coupling through two bonds. The magnitudes of the latter coupling are not sufficient to allow the two separate contributions from ^{107}Ag and ^{109}Ag to be resolved. The ^{31}P-{^{1}H} n.m.r. spectrum of (**10**) is still slightly broadened by the dynamic behaviour of the cluster at −100 °C and the splittings due to $^{2}J(^{107,109}\mathrm{Ag}\text{–}^{31}\mathrm{P})$ cannot be resolved. The high-field ^{1}H n.m.r. hydrido ligand signals of (**9**)—(**14**) all appear to be triplets of triplets of triplets (Figure 5). However, the patterns actually consist of three superimposed subspectra, due to the different isotopomers that are possible from the

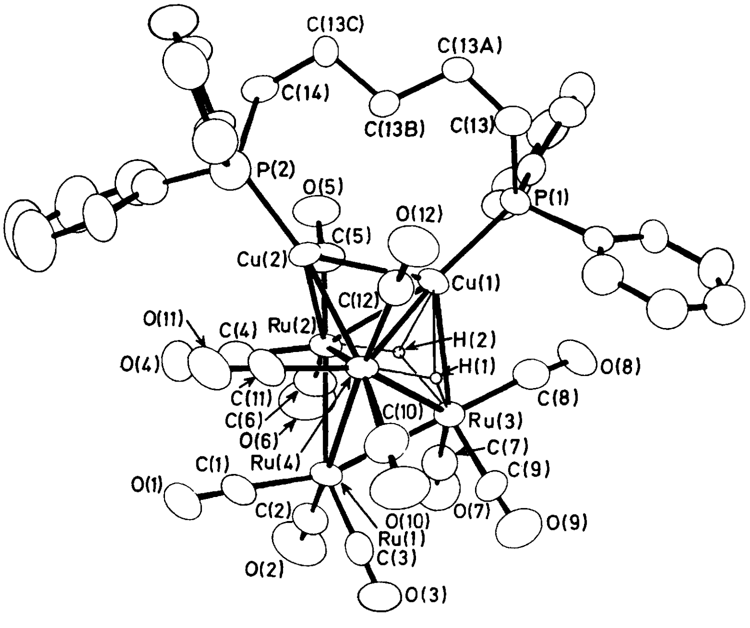

Figure 3. Molecular structure of $[Cu_2Ru_4(\mu_3\text{-}H)_2\{\mu\text{-}Ph_2P(CH_2)_5PPh_2\}(CO)_{12}]$ (**7**), showing the crystallographic numbering

Table 3. Selected bond lengths (Å), with estimated standard deviations in parentheses, for $[Cu_2Ru_4(\mu_3\text{-}H)_2\{\mu\text{-}Ph_2P(CH_2)_nPPh_2\}(CO)_{12}]$ [n = 2, (**4**), 3 (**5**), or 5 (**7**)]

	(**4**)			
	A	B	(**5**)	(**7**)
Ru(1)–Ru(2)	2.801(2)	2.790(2)	2.789(1)	2.798(1)
Ru(1)–Ru(3)	2.800(2)	2.792(2)	2.788(1)	2.787(1)
Ru(1)–Ru(4)	2.800(2)	2.795(2)	2.791(1)	2.801(1)
Ru(1)–C(1)	1.89(2)	1.86(2)	1.914(12)	1.832(7)
Ru(1)–C(2)	1.90(2)	1.94(2)	1.904(10)	1.924(6)
Ru(1)–C(3)	1.80(2)	1.93(2)	1.906(10)	1.852(6)
Ru(2)–Ru(3)	2.957(2)	2.963(2)	2.955(1)	2.944(1)
Ru(2)–Ru(4)	2.887(2)	2.895(2)	2.915(1)	2.916(1)
Ru(2)–Cu(1)	2.813(2)	2.788(2)	2.743(1)	2.792(1)
Ru(2)–Cu(2)	2.616(2)	2.654(2)	2.649(1)	2.624(1)
Ru(2)–C(4)	1.84(2)	1.94(2)	1.933(9)	1.862(7)
Ru(2)–C(5)	1.84(2)	1.83(2)	1.936(10)	1.915(6)
Ru(2)–C(6)	1.97(2)	1.93(2)	1.850(13)	1.909(6)
Ru(2)–H(2)	2.05	1.87	1.01	1.36
Ru(3)–Ru(4)	2.956(2)	2.977(2)	2.961(1)	2.986(1)
Ru(3)–Cu(1)	2.652(3)	2.699(3)	2.742(1)	2.782(1)
Ru(3)–C(7)	1.92(2)	1.88(2)	1.915(11)	1.896(6)
Ru(3)–C(8)	1.95(2)	1.82(2)	1.863(14)	1.918(7)
Ru(3)–C(9)	1.90(2)	1.91(2)	1.885(10)	1.856(7)
Ru(3)–H(1)	2.05	2.17	2.64	1.94
Ru(3)–H(2)	1.0	1.26	2.44	1.89
Ru(4)–Cu(1)	2.708(3)	2.748(3)	2.693(1)	2.682(1)
Ru(4)–Cu(2)	2.615(3)	2.603(3)	2.647(1)	2.623(2)
Ru(4)–C(10)	1.81(2)	1.91(2)	1.822(12)	1.885(7)
Ru(4)–C(11)	1.88(2)	1.93(2)	1.901(9)	1.859(7)
Ru(4)–C(12)	1.90(2)	1.92(2)	1.959(9)	1.925(5)
Ru(4)–H(1)	1.24	1.12	1.11	1.38
Cu(1)–Cu(2)	2.505(3)	2.492(3)	2.568(1)	2.659(1)
Cu(1)–P(1)	2.222(7)	2.189(7)	2.213(2)	2.236(1)
Cu(1)–H(1)	1.79	1.77	2.09	1.85
Cu(1)–H(2)	1.97	1.83	1.94	2.28
O(3)–C(3)	1.18(3)	1.14(2)	1.141(10)	1.160(6)
O(4)–C(4)	1.17(2)	1.14(2)	1.129(10)	1.169(7)
O(5)–C(5)	1.15(2)	1.18(2)	1.121(11)	1.143(6)
O(6)–C(6)	1.13(2)	1.07(2)	1.178(13)	1.129(6)
O(7)–C(7)	1.12(2)	1.14(2)	1.125(11)	1.123(6)
O(8)–C(8)	1.10(2)	1.15(3)	1.215(14)	1.157(7)
O(9)–C(9)	1.12(2)	1.18(2)	1.128(11)	1.154(7)
O(10)–C(10)	1.21(2)	1.13(2)	1.188(12)	1.161(7)
O(11)–C(11)	1.15(2)	1.15(2)	1.125(10)	1.166(7)
O(12)–C(12)	1.15(2)	1.15(2)	1.121(10)	1.140(6)
C(13)–C(13A)			1.527(12)	1.500(8)
C(13)–C(14)	1.54(3)	1.54(3)		
C(13A)–C(14)			1.508(12)	
C(13A)–C(13B)				1.518(7)
C(13B)–C(13C)				1.489(7)
C(13C)–C(14)				1.524(8)
Cu(2)–P(2)	2.238(7)	2.176(7)	2.224(2)	2.224(1)
P(1)–C(13)	1.79(2)	1.85(2)	1.821(8)	1.847(1)
P(1)–C(15)	1.866(15)	1.83(2)	1.815(9)	1.854(1)
P(1)–C(21)	1.77(2)	1.80(2)	1.814(8)	1.803(1)
P(2)–C(14)	1.81(2)	1.80(2)	1.856(8)	1.850(1)
P(2)–C(27)	1.80(2)	1.82(2)	1.819(8)	1.813(1)
P(2)–C(33)	1.83(2)	1.84(2)	1.825(8)	1.824(1)
O(1)–C(1)	1.06(2)	1.17(2)	1.087(11)	1.181(7)
O(2)–C(2)	1.17(3)	1.17(2)	1.156(10)	1.126(6)
Cu(1)–C(8)	2.81(2)	2.84(2)	2.83(1)	>3
Cu(1)–C(12)	2.86(2)	2.87(2)	2.82(1)	2.744(6)
Cu(2)–C(4)	3.04(2)	2.93(2)	2.73(1)	2.882(6)
Cu(2)–C(5)	2.57(2)	2.56(2)	2.84(1)	2.585(6)
Cu(2)–C(11)	2.56(2)	2.73(2)	2.82(1)	2.711(6)
Cu(2)–C(12)	2.91(2)	2.92(2)	2.84(1)	2.719(6)

Table 4. Selected bond angles (°), with estimated standard deviations in parentheses, for $[Cu_2Ru_4(\mu_3\text{-}H)_2\{\mu\text{-}Ph_2P(CH_2)_nPPh_2\}(CO)_{12}]$ [n = 2 (**4**), 3 (**5**), or 5 (**7**)]

	(**4**)			
	A	B	(**5**)	(**7**)
Ru(2)–Ru(1)–Ru(3)	63.72(5)	64.13(6)	64.00(2)	63.63(2)
Ru(2)–Ru(1)–Ru(4)	62.06(5)	62.44(5)	62.98(2)	62.79(1)
Ru(2)–Ru(1)–C(1)	103.6(1)	98.8(1)	93.94(6)	105.4(2)
Ru(2)–Ru(1)–C(2)	101.6(1)	98.5(2)	102.23(6)	99.6(2)
Ru(2)–Ru(1)–C(3)	160.3(1)	160.9(1)	159.92(7)	156.5(2)
Ru(3)–Ru(1)–Ru(4)	64.69(5)	64.39(5)	64.13(2)	64.60(2)
Ru(3)–Ru(1)–C(1)	161.0(1)	156.6(1)	156.57(7)	161.5(2)
Ru(3)–Ru(1)–C(2)	101.3(1)	101.8(2)	97.87(6)	103.1(2)
Ru(3)–Ru(1)–C(3)	98.8(1)	98.6(1)	103.63(8)	94.9(2)
Ru(4)–Ru(1)–C(1)	97.2(1)	94.1(1)	99.91(6)	97.4(2)
Ru(4)–Ru(1)–C(2)	161.6(2)	159.6(1)	159.96(7)	161.3(2)
Ru(4)–Ru(1)–C(3)	103.3(1)	104.0(2)	97.78(7)	100.3(2)
C(1)–Ru(1)–C(2)	94.9(8)	96.2(9)	94.3(4)	93.2(2)
C(1)–Ru(1)–C(3)	90.6(9)	95.2(8)	95.1(5)	92.4(2)
C(2)–Ru(1)–C(3)	90.2(9)	92.6(9)	94.9(4)	94.5(2)
Ru(1)–Ru(2)–Ru(3)	58.12(5)	57.97(5)	57.97(2)	58.02(1)
Ru(1)–Ru(2)–Ru(4)	58.96(5)	58.86(5)	58.55(2)	58.67(1)
Ru(1)–Ru(2)–Cu(1)	101.49(7)	103.09(7)	103.44(3)	103.11(2)
Ru(1)–Ru(2)–Cu(2)	112.94(8)	111.88(8)	110.63(3)	109.26(2)
Ru(1)–Ru(2)–C(4)	89.0(1)	88.8(2)	82.31(7)	79.6(2)
Ru(1)–Ru(2)–C(5)	82.9(1)	83.1(1)	90.20(7)	89.4(2)
Ru(1)–Ru(2)–C(6)	178.0(1)	177.6(2)	172.69(6)	176.6(2)
Ru(1)–Ru(2)–H(2)	65	69	108	85
Ru(3)–Ru(2)–Ru(4)	61.67(5)	61.06(5)	60.59(2)	61.27(1)
Ru(3)–Ru(2)–Cu(1)	54.65(6)	55.87(6)	57.38(3)	57.95(2)
Ru(3)–Ru(2)–Cu(2)	102.84(7)	102.32(7)	105.52(3)	107.55(2)
Ru(3)–Ru(2)–C(4)	95.8(1)	96.3(1)	94.64(7)	95.7(2)
Ru(3)–Ru(2)–C(5)	139.5(2)	138.9(2)	145.99(7)	136.9(2)
Ru(3)–Ru(2)–C(6)	120.1(1)	122.7(1)	116.44(6)	123.3(2)
Cu(1)–Ru(2)–Cu(2)	54.80(7)	54.52(7)	56.85(3)	58.71(2)
Cu(1)–Ru(2)–C(4)	131.5(1)	131.7(1)	137.39(7)	133.9(2)
Cu(1)–Ru(2)–C(5)	133.5(1)	132.1(1)	129.26(7)	135.1(2)
Cu(1)–Ru(2)–C(6)	76.6(2)	76.2(1)	75.21(6)	76.0(2)
Cu(1)–Ru(2)–H(2)	44	49	31	54
Cu(2)–Ru(2)–C(4)	156.5(1)	157.4(1)	159.64(7)	155.5(2)
Cu(2)–Ru(2)–C(5)	80.7(1)	78.8(2)	72.52(6)	77.9(2)
Cu(2)–Ru(2)–C(6)	66.2(1)	65.8(1)	74.89(7)	67.4(1)
Cu(2)–Ru(2)–H(2)	93	89	84	113
C(4)–Ru(2)–C(5)	94.4(8)	95.5(9)	93.0(4)	90.5(3)
C(4)–Ru(2)–H(2)	105	108	107	97
C(4)–Ru(2)–C(6)	92.1(9)	93.3(8)	93.4(5)	93.6(2)
C(5)–Ru(2)–C(6)	98.5(8)	95.7(9)	96.5(4)	98.7(2)
C(5)–Ru(2)–H(2)	141	143	154	164
C(6)–Ru(2)–H(2)	114	111	67	84
Ru(1)–Ru(3)–Ru(2)	58.15(5)	57.90(5)	58.02(2)	58.35(1)
Ru(1)–Ru(3)–Ru(4)	57.66(5)	57.86(5)	57.99(2)	57.92(1)
Ru(1)–Ru(3)–Cu(1)	105.73(8)	105.39(7)	103.52(3)	103.64(2)
Ru(1)–Ru(3)–C(7)	81.5(1)	81.3(2)	87.15(6)	82.1(2)
Ru(1)–Ru(3)–C(8)	177.7(2)	178.4(2)	174.53(7)	174.6(2)
Ru(1)–Ru(3)–C(9)	86.9(2)	87.2(1)	81.02(6)	88.2(2)
Ru(1)–Ru(3)–H(1)	76	75	80	79
Ru(1)–Ru(3)–H(2)	72	75	77	77
Ru(2)–Ru(3)–Ru(4)	58.03(5)	58.33(5)	59.03(2)	58.91(1)
Ru(2)–Ru(3)–Cu(1)	59.91(6)	58.77(6)	57.42(3)	58.29(2)
Ru(2)–Ru(3)–C(7)	93.3(1)	93.5(2)	94.77(6)	92.4(2)
Ru(2)–Ru(3)–C(8)	119.9(1)	123.7(1)	121.72(7)	118.6(2)
Ru(2)–Ru(3)–C(9)	143.6(2)	143.0(1)	138.14(7)	145.0(2)
Ru(2)–Ru(3)–H(1)	66	60	73	69

Table 4 (*continued*)

	(4)		(5)	(7)
	A	B		
Ru(3)–Ru(2)–H(2)	11	15	51	30
Ru(4)–Ru(2)–Cu(1)	56.72(6)	57.81(6)	56.76(3)	56.00(2)
Ru(4)–Ru(2)–Cu(2)	56.48(6)	55.74(6)	56.59(3)	56.23(3)
Ru(4)–Ru(2)–C(4)	146.9(1)	146.6(2)	140.30(6)	146.8(2)
Ru(4)–Ru(2)–C(5)	89.8(1)	88.9(1)	93.87(7)	91.9(2)
Ru(4)–Ru(2)–C(6)	119.5(1)	119.2(1)	124.25(7)	118.7(1)
Ru(4)–Ru(2)–H(2)	44	56	82	85
Cu(1)–Ru(3)–C(7)	137.9(1)	136.5(2)	133.37(6)	136.5(2)
Cu(1)–Ru(3)–C(8)	73.4(2)	76.0(2)	73.21(6)	77.0(2)
Cu(1)–Ru(3)–C(9)	130.3(1)	129.9(1)	135.01(2)	129.9(2)
Cu(1)–Ru(3)–H(1)	43	41	46	41
Cu(1)–Ru(3)–H(2)	39	36	44	54
C(7)–Ru(3)–C(8)	97.8(9)	98.3(8)	97.9(4)	93.7(2)
C(7)–Ru(3)–C(9)	90.9(9)	92.8(9)	91.0(5)	93.0(3)
C(7)–Ru(3)–H(1)	104	151	165	159
C(7)–Ru(3)–H(2)	106	146	99	86
C(8)–Ru(3)–C(9)	95.2(8)	91.3(8)	98.2(5)	95.5(3)
C(8)–Ru(3)–H(1)	104	106	95	104
C(8)–Ru(3)–H(2)	106	112	103	99
C(9)–Ru(3)–H(1)	99	102	93	96
C(9)–Ru(3)–H(2)	146	107	155	165
H(1)–Ru(3)–H(2)	49	45	72	80
Ru(1)–Ru(4)–Ru(2)	58.98(4)	58.69(5)	58.48(2)	58.55(1)
Ru(1)–Ru(4)–Ru(3)	57.65(5)	57.76(5)	57.88(2)	57.48(1)
Ru(1)–Ru(4)–Cu(1)	104.20(6)	103.99(7)	104.70(3)	105.93(2)
Ru(1)–Ru(4)–Cu(2)	112.99(7)	113.34(7)	110.61(3)	109.16(2)
Ru(1)–Ru(4)–C(10)	88.3(2)	88.5(1)	85.28(7)	83.9(2)
Ru(1)–Ru(4)–C(11)	84.5(1)	78.5(1)	88.16(7)	86.3(2)
Ru(1)–Ru(4)–C(12)	179.8(2)	172.8(2)	177.32(6)	176.3(2)
Ru(1)–Ru(4)–H(1)	89	92	119	88
Ru(2)–Ru(4)–Ru(3)	60.30(5)	60.60(5)	60.38(2)	59.82(1)
Ru(2)–Ru(4)–Cu(1)	60.25(6)	59.14(6)	58.41(3)	59.66(2)
Ru(2)–Ru(4)–Cu(2)	56.51(6)	57.44(6)	56.64(3)	56.24(2)
Ru(2)–Ru(4)–C(10)	93.9(2)	94.2(2)	92.86(6)	92.7(2)
Ru(2)–Ru(4)–C(11)	142.0(2)	137.2(1)	145.58(6)	141.8(2)
Ru(2)–Ru(4)–C(12)	120.6(2)	137.2(1)	119.98(6)	120.2(2)
Ru(2)–Ru(4)–H(1)	74	66	103	76
Ru(3)–Ru(4)–Cu(1)	55.12(6)	56.08(6)	57.77(3)	58.49(2)
Ru(3)–Ru(4)–Cu(2)	101.81(7)	103.24(7)	105.39(3)	106.34(2)
Ru(3)–Ru(4)–C(10)	144.1(2)	144.6(2)	141.69(6)	141.9(2)
Ru(3)–Ru(4)–C(11)	92.7(1)	95.7(2)	96.19(6)	95.7(2)
Ru(3)–Ru(4)–C(12)	121.2(1)	117.8(2)	119.51(6)	118.8(2)
Ru(3)–Ru(4)–H(1)	32	36	44	31
Ru(2)–Cu(2)–Ru(4)	67.00(7)	66.82(7)	66.78(3)	67.53(2)
Ru(2)–Cu(2)–Cu(1)	66.60(8)	65.44(7)	63.43(3)	63.81(2)
Ru(2)–Cu(2)–P(2)	135.8(2)	134.9(2)	142.46(7)	136.51(4)
Ru(4)–Cu(2)–Cu(1)	63.84(8)	65.12(8)	62.17(3)	61.03(2)
Ru(4)–Cu(2)–P(2)	155.8(2)	157.87(2)	148.69(7)	149.49(4)
Cu(1)–Cu(2)–P(2)	113.4(2)	115.85(2)	132.09(7)	139.62(5)
C(13)–P(1)–C(15)	104.9(9)	101.6(8)	103.7(4)	101.7(2)
C(13)–P(1)–C(21)	101.8(9)	104.7(9)	105.1(4)	104.0(2)
C(15)–P(1)–C(21)	104.4(8)	101.5(9)	104.2(4)	104.4(2)
Cu(2)–P(2)–C(14)	109.3(4)	109.6(4)	113.4(2)	114.4(1)
Cu(2)–P(2)–C(27)	116.3(4)	120.3(5)	109.2(1)	109.9(2)
Cu(2)–P(2)–C(33)	116.5(5)	112.9(5)	117.8(1)	116.8(2)
C(14)–P(2)–C(27)	104.6(9)	103.3(9)	104.5(4)	104.7(2)
C(14)–P(2)–C(33)	101.8(8)	107(1)	106.0(4)	105.2(2)
C(27)–P(2)–C(33)	105.1(9)	105.3(9)	105.0(4)	104.8(2)
Ru(3)–C(9)–O(9)	179(2)	170(2)	177(1)	175.7(8)
Ru(4)–C(10)–O(10)	170(2)	171(2)	177.9(9)	176.1(8)
Ru(4)–C(11)–O(11)	173(2)	170(2)	176.0(8)	176.8(8)
Ru(4)–C(12)–O(12)	169(2)	174(2)	173.0(7)	169.4(9)
P(1)–C(13)–C(13A)			113.4(6)	115.8(5)
Ru(2)–Ru(3)–H(2)	22	23	19	21
Ru(4)–Ru(3)–Cu(1)	56.92(7)	57.68(6)	56.20(3)	55.28(2)
Ru(4)–Ru(3)–C(7)	137.9(1)	138.0(1)	143.47(6)	138.5(2)
Ru(4)–Ru(3)–C(8)	122.6(2)	122.8(2)	116.78(6)	125.3(2)
Ru(4)–Ru(3)–C(9)	96.3(2)	94.2(1)	93.48(7)	96.0(2)
Ru(4)–Ru(3)–H(1)	19	18	22	21
Ru(4)–Ru(3)–H(2)	48	51	65	75
Cu(1)–Ru(4)–Cu(2)	56.10(8)	55.52(8)	57.47(3)	60.15(2)
Cu(1)–Ru(4)–C(10)	135.8(1)	138.5(2)	133.14(7)	134.9(2)
Cu(1)–Ru(4)–C(11)	127.6(2)	134.2(1)	132.67(6)	132.4(2)
Cu(1)–Ru(4)–C(12)	74.64(1)	75.7(2)	72.72(6)	71.0(2)
Cu(1)–Ru(4)–H(1)	33	24	58	40
Cu(2)–Ru(4)–C(10)	79.8(2)	78.9(1)	76.00(7)	72.4(2)
Cu(2)–Ru(4)–C(11)	161.4(1)	160.9(2)	156.71(6)	157.9(2)
Cu(2)–Ru(4)–C(12)	66.8(2)	72.6(9)	68.94(2)	71.3(2)
Cu(2)–Ru(4)–H(1)	89	79	113	99
C(10)–Ru(4)–C(11)	95.2(8)	86.9(1)	92.6(4)	91.3(3)
C(10)–Ru(4)–C(12)	92.8(9)	97.7(8)	93.0(3)	96.9(2)
C(10)–Ru(4)–H(1)	167	156	87	168
C(11)–Ru(4)–C(12)	95.8(8)	96.8(8)	97.3(4)	97.3(2)
C(11)–Ru(4)–H(1)	97	117	156	99
C(12)–Ru(4)–H(1)	89	85	58	88
Ru(2)–Cu(1)–Ru(3)	65.43(6)	65.36(6)	65.20(3)	63.77(2)
Ru(2)–Cu(1)–Ru(4)	63.03(6)	63.05(6)	64.83(3)	64.34(2)
Ru(2)–Cu(1)–Cu(2)	58.59(7)	60.06(6)	59.72(3)	57.48(2)
Ru(2)–Cu(1)–P(1)	141.3(2)	139.9(2)	141.91(7)	152.20(5)
Ru(2)–Cu(1)–H(1)	71	66	86	74
Ru(2)–Cu(1)–H(2)	47	42	15	29
Ru(3)–Cu(1)–Ru(4)	67.96(7)	66.29(6)	66.02(3)	66.23(2)
Ru(3)–Cu(1)–Cu(2)	115.5(1)	115.0(1)	114.44(4)	111.40(3)
Ru(3)–Cu(1)–P(1)	143.3(2)	145.5(2)	143.29(7)	125.55(4)
Ru(3)–Cu(1)–H(1)	51	53	65	44
Ru(3)–Cu(1)–H(2)	19	24	60	42
Ru(4)–Cu(1)–Cu(2)	60.07(8)	59.38(8)	60.36(3)	58.83(2)
Ru(4)–Cu(1)–P(1)	138.9(2)	139.2(2)	138.99(7)	142.60(4)
Ru(4)–Cu(1)–H(1)	22	15	23	28
Ru(4)–Cu(1)–H(2)	61	59	77	77
Cu(2)–Cu(1)–P(1)	100.9(2)	99.5(2)	102.27(7)	123.00(4)
Cu(2)–Cu(1)–H(1)	82	74	78	87
Cu(2)–Cu(1)–H(2)	98	95	73	86
P(1)–Cu(1)–H(1)	143	145	126	132
P(1)–Cu(1)–H(2)	158	161	137	138
H(1)–Cu(1)–H(2)	49	51	96	72
C(13)–C(13A)–C(13B)				114.0(4)
C(13A)–C(13B)–C(13C)				116.5(4)
C(13B)–C(13C)–C(14)				113.8(4)
P(2)–C(14)–C(13C)				113.3(2)
Cu(1)–P(1)–C(13)	118.7(5)	117.6(5)	111.3(1)	119.9(1)
Cu(1)–P(1)–C(15)	110.4(4)	116.1(4)	117.4(1)	110.0(1)
Cu(1)–P(1)–C(21)	115.7(5)	113.9(4)	114.1(2)	115.2(1)
Ru(1)–C(1)–O(1)	180(1)	172(2)	175.4(9)	178.3(7)
Ru(1)–C(2)–O(2)	171(2)	177(2)	177.3(8)	177.1(8)
Ru(1)–C(3)–O(3)	174(2)	176(2)	176.4(9)	178.4(8)
Ru(2)–C(4)–O(4)	172(2)	174(2)	171.5(7)	175.4(7)
Ru(2)–C(5)–O(5)	178(2)	173(2)	172.2(9)	171.1(8)
Ru(2)–C(6)–O(6)	172(2)	170(2)	176.4(9)	176.3(8)
Ru(3)–C(7)–O(7)	173(2)	173(2)	176.5(9)	175.5(7)
Ru(3)–C(8)–O(8)	168(2)	173(2)	172.2(9)	170.9(8)
P(1)–C(13)–C(14)	118(1)	115(1)		
C(13)–C(13A)–C(14)			116.5(7)	
P(2)–C(14)–C(13A)			113.1(5)	
P(2)–C(14)–C(13)	116(1)	111(1)		

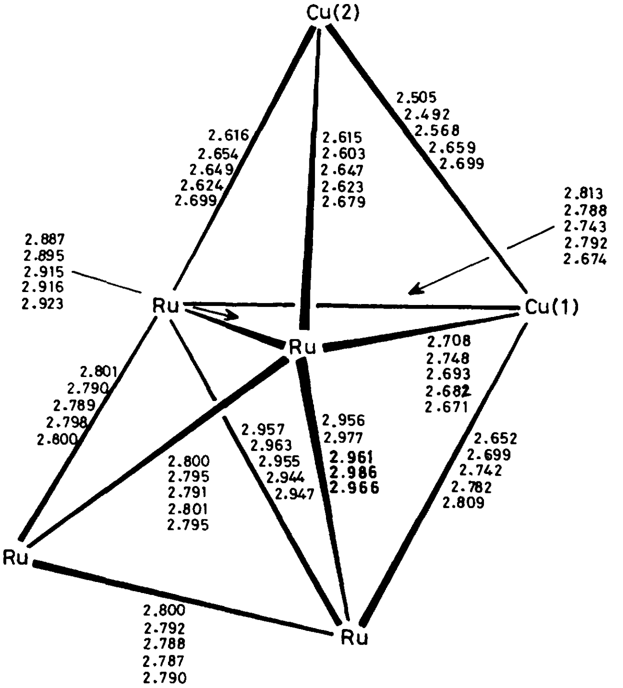

Figure 4. A comparison of the metal–metal separations (Å) within the capped trigonal-bipyramidal metal cores of $[Cu_2Ru_4(\mu_3\text{-}H)_2L_2(CO)_{12}]$ [L = PPh_3 (**1**) or L_2 = $\mu\text{-}Ph_2P(CH_2)_nPPh_2$, n = 2 (**4**), 3 (**5**), or 5 (**7**)]. Distances are given in the following descending order: molecule A of (**4**), molecule B of (**4**), (**5**), (**7**), and (**1**)[3]

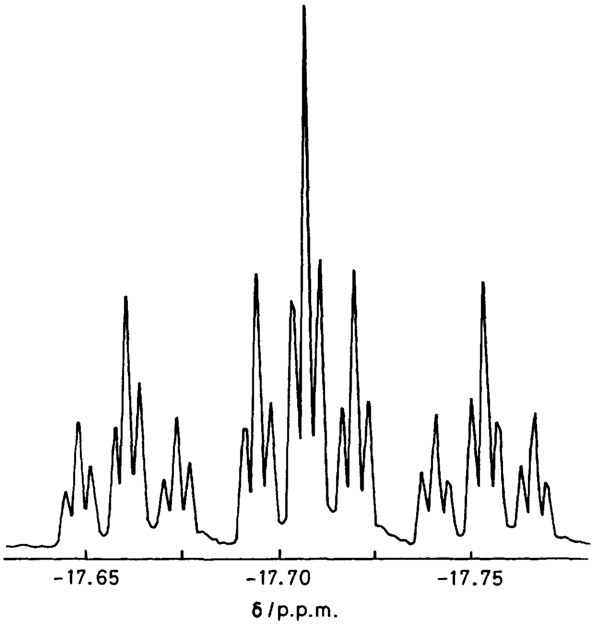

Figure 5. The high-field hydrido ligand signal in the ambient-temperature ^1H n.m.r. spectrum of $[Ag_2Ru_4(\mu_3\text{-}H)_2(\mu\text{-}Ph_2PCH_2PPh_2)(CO)_{12}]$ (**9**)

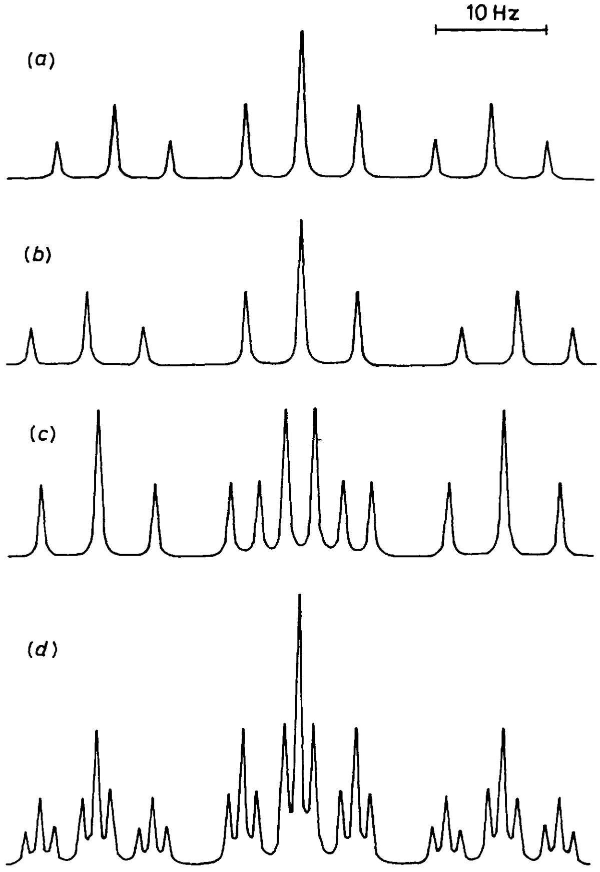

Figure 6. Simulations of the high-field hydrido ligand signal in the ^1H n.m.r. spectrum of $[Ag_2Ru_4(\mu_3\text{-}H)_2(\mu\text{-}Ph_2PCH_2PPh_2)(CO)_{12}]$ (**9**). (*a*) Subspectrum for the $^{107}Ag^{107}Ag$ isotopomer, (*b*) subspectrum for the $^{109}Ag^{109}Ag$ isotopomer, (*c*) subspectrum for the $^{107}Ag^{109}Ag$ isotopomer, and (*d*) total spectrum

various combinations of the two naturally occurring isotopes of silver (^{107}Ag and ^{109}Ag). The subspectra are split by $^{107,109}Ag\text{–}^1H$ and $^{31}P\text{–}^1H$ couplings and when they are summed together, with the appropriate statistical weightings for the relative isotopic abundances, the triplet of triplets of triplets pattern is produced (Figure 6). At low temperatures, the ^1H n.m.r. hydrido ligand signals of (**11**)—(**14**) all show couplings to one silver atom and one phosphorus atom, as expected,[3] but only the $^{107,109}Ag\text{–}^1H$ coupling can be resolved for (**10**) at −100 °C, as the peak is still somewhat broadened by the dynamic behaviour. In the case of (**9**), a ^1H n.m.r. spectrum consistent with the ground-state structure could not be obtained and the pattern of the hydrido ligand resonance at −100 °C is very similar to that observed at ambient temperature, although the signals are slightly broadened.

The variable-temperature n.m.r. data clearly demonstrate that (**3**)—(**14**), like the PPh_3 clusters (**1**) and (**2**),[3] undergo dynamic behaviour which exchanges the phosphorus atoms between the two distinct sites in the ground-state structures. As in the case of (**1**) and (**2**),[3] an intramolecular rearrangement of the actual metal skeletons of (**3**)—(**14**) seems to be the only reasonable explanation for the n.m.r. results. Thus, the two Group 1B metals in a capped trigonal-bipyramidal M_2Ru_4 (M = Cu or Ag) metal skeleton can still undergo site-exchange even when they are linked together by the bidentate diphosphine ligands $Ph_2P(CH_2)_nPPh_2$ (n = 1—6).

Experimental

The techniques used and the instrumentation employed have been described elsewhere.[12] Light petroleum refers to that fraction of b.p. 40—60 °C. Established methods were used to prepare the salt $[N(PPh_3)_2]_2[Ru_4(\mu\text{-}H)_2(CO)_{12}]$[17] and the complex $[Cu(NCMe)_4]PF_6$.[18] The compound $[Ag(NCMe)_4]PF_6$ was synthesized by an adaptation of the published

Table 5. Quantities of diphosphine ligand used and product obtained and the chromatography conditions employed for the synthesis of clusters $[M_2Ru_4(\mu_3\text{-}H)_2\{\mu\text{-}Ph_2P(CH_2)_nPPh_2\}(CO)_{12}]$ (M = Cu or Ag, n = 1—6)

n	Quantity of $Ph_2P(CH_2)_n$-PPh_2 used/g (mmol)	Quantity of product obtained/g		Proportions of dichloromethane–light petroleum used for elution[a]	
		M = Cu	M = Ag	M = Cu[b]	M = Ag[c]
1	0.26 (0.68)	0.56	0.64	1:1	2:3
2	0.27 (0.68)	0.58	0.60	1:1	2:3
3	0.28 (0.68)	0.59	0.64	1:1	1:1
4	0.29 (0.68)	0.62	0.71	3:2	3:2
5	0.30 (0.68)	0.58	0.63	2:1	2:1
6	0.31 (0.68)	0.52	0.63	2:1	3:1

[a] The crude product was initially dissolved in the same solvent mixture as that used for elution. [b] The chromatography was performed on a Florisil column (20 × 3 cm) at −20 °C. [c] The chromatography was performed on an alumina column (20 × 3 cm) at −20 °C.

Table 6. Crystal structure analysis of (**4**), (**5**), and (**7**)

Complex	(**4**)·CH_2Cl_2	(**5**)·CH_2Cl_2	(**7**)·CH_2Cl_2
Data collection[a]			
Crystal colour and habit	red plate	red plate	red plate
Crystal size/mm	0.1 × 0.3 × 0.3	0.1 × 0.2 × 0.2	0.15 × 0.2 × 0.2
2θ range/°	0—50	0—50	0—50
Scan method	ω/2θ = 1	ω/2θ = 1	ω/2θ = 1
$t_{max.}$/s	60	60	60
No. of unique data	8 375	9 015	8 602
R_{int}	0.028	0.025	0.029
No of 'observed' data (n.o.)	4 967	5 556	4 887
'Observed' criterion, n [$I > n\sigma(I)$]	1	2	3
Structure solution and refinement[b]			
Anisotropic atoms	Cu,Ru,O,P,C	Cu,Ru,O,P,C	Cu,Ru,O,P,C
Isotropic atoms	CH_2Cl_2 and hydride H	CH_2Cl_2 and hydride H	CH_2Cl_2 and hydride H
No. of variables (n.v.)	535	587	578
R[c]	0.058	0.075	0.039
R'	0.057	0.061	0.033
S	1.6	2.8	1.7
Largest final difference electron density features (e Å^{-3})	0.69	0.44	0.35

[a] Data were collected at 293 K on an Enraf-Nonius automatic CAD-4 diffractometer. During data collection the time of measurement and scan speed are variable and $t_{max.}$ gives the limit to the time of measurement. [b] The structures were solved by MULTAN and Fourier difference syntheses. All of the calculations were computed on a Digital PDP 11/60 computer with the SDP package (Frenz). [c] $R = \Sigma||F_o| - |F_c||/\Sigma|F_o|$; $R' = \Sigma w^{\frac{1}{2}}||F_o| - |F_c||/\Sigma w^{\frac{1}{2}}|F_o|$; $S = [\Sigma w(|F_o| - |F_c|)^2/\Sigma(\text{n.o.} - \text{n.v.})]^{\frac{1}{2}}$.

route.[18,19] The bidentate diphosphine ligands $Ph_2P(CH_2)_n$-PPh_2 (n = 1—6) were purchased from Strem Chemicals Inc., and used without further purification. Analytical and other physical data for the new compounds are presented in Table 1, together with their i.r. spectra, and Table 2 summarizes the results of n.m.r. spectroscopic measurements. Product separation by column chromatography was performed on Aldrich Florisil (100—200 mesh) or B.D.H. alumina (Brockman activity II).

Synthesis of the Compounds $[M_2Ru_4(\mu_3\text{-}H)_2\{\mu\text{-}Ph_2P(CH_2)_nPPh_2\}(CO)_{12}]$ (M = Cu *or* Ag, n = 1—6).—A dichloromethane (70 cm^3) solution of $[N(PPh_3)_2]_2[Ru_4(\mu\text{-}H)_2(CO)_{12}]$ (1.20 g, 0.66 mmol) at −30 °C was treated with a solution of $[M(NCMe)_4]PF_6$ (M = Cu, 0.49 g, 1.32 mmol; M = Ag, 0.55 g, 1.32 mmol) in dichloromethane (50 cm^3) and then, after stirring the reaction mixture at −30 °C for 1 min, a dichloromethane (30 cm^3) solution containing an appropriate amount (Table 5) of the desired diphosphine ligand was added. The mixture was allowed to warm to ambient temperature with stirring and the solvent was then removed under reduced pressure. The residue was extracted with dichloromethane–diethyl ether (1:4; 50 cm^3 portions) until the extracts were no longer red and the combined extracts were then filtered through a Celite pad (*ca.* 1 × 3 cm). After removal of the solvent under reduced pressure, the crude residue was dissolved and chromatographed, using the appropriate conditions (Table 5). The chromatography afforded one dark red fraction, which, after removal of the solvent under reduced pressure and crystallization of the residue from dichloromethane–light petroleum, yielded dark red *microcrystals* of the product. Table 5 lists the amounts of (**3**)—(**14**) obtained.

Crystal Structure Determinations for (**4**)·CH_2Cl_2, (**5**)·CH_2Cl_2, *and* (**7**)·CH_2Cl_2.—Suitable crystals of the three clusters were grown from dichloromethane–diethyl ether–light petroleum by slow layer diffusion at −20 °C.

Crystal data for (**4**)·CH_2Cl_2. $C_{38}H_{26}Cu_2O_{12}P_2Ru_4\cdot CH_2Cl_2$, M = 1 351.9, monoclinic, space group $P2_1$, a = 12.689(5), b = 27.589(6), c = 13.759(3) Å, β = 104.97(5)°, U = 4 653(1) Å^3, Z = 4, D_c = 1.93 g cm^{-3}, λ(Mo-K_α) = 0.710 73 Å, μ(Mo-K_α) = 23.82 cm^{-1}, F(000) = 3 608.

For (**5**)·CH_2Cl_2.$C_{39}H_{28}Cu_2O_{12}P_2Ru_4\cdot CH_2Cl_2$, M = 1 365.9, monoclinic, space group $P2_1/n$, a = 14.024(5), b = 16.799(7), c = 21.994(6) Å, β = 101.94(7)°, U = 5 069 Å^3, Z = 4, D_c = 1.79 g cm^{-3}, λ(Mo-K_α) = 0.710 73 Å, μ(Mo-K_α) = 21.87 cm^{-1}, F(000) = 3 640.

For (**7**)·CH_2Cl_2. $C_{41}H_{32}Cu_2O_{12}P_2Ru_4\cdot CH_2Cl_2$, M = 1 393.9, monoclinic, space group $P2_1/c$, a = 11.864(3), b = 26.047(5), c = 16.445(4) Å, β = 105.24(7)°, U = 4 903 Å^3, Z = 4, D_c = 1.89 g cm^{-3}, λ(Mo-K_α) = 0.710 73 Å, μ(Mo-K_α) = 22.64 cm^{-1}, F(000) = 3 704.

Table 6 lists important details of the structure determinations of (**4**)·CH_2Cl_2, (**5**)·CH_2Cl_2, and (**7**)·CH_2Cl_2. In each case, crystals were sealed, under N_2, in thin-walled glass capillaries for *X*-ray measurements.

The structures of (**4**), (**5**), and (**7**) were solved by direct methods (MULTAN). Two independent clusters in a nearly centrosymmetric space group were revealed in (**4**) and, after several refinements and Fourier difference syntheses, two CH_2Cl_2 sites, with occupancies of *ca.* 0.5 were also found. The two independent molecules of (**4**) were refined alternately, because a complete refinement would involve correlations in the matrix due to pseudo-symmetry. For (**5**) and (**7**), the positions of the Cu, Ru, and P atoms were found by direct methods. Successive refinements and Fourier difference syntheses revealed the locations of the remaining atoms and also one molecule of CH_2Cl_2 in each case. It was possible to find some of the hydrogen atoms of the bidentate diphosphine ligands attached to (**4**), (**5**), and (**7**) after isotropic and anisotropic refinements, but all of these hydrogen atoms have been set in calculated positions for each cluster. After a full-matrix least-squares refinement of all of the non-hydrogen atoms in (**4**), (**5**), and (**7**), the highest peaks of the Fourier difference maps occur at the positions of the expected triply bridging hydrido ligands, but refinement of their co-ordinates was not possible without constraint. Final positional parameters for refined atoms are given in Tables 7, 8, and 9 for (**4**)·CH_2Cl_2, (**5**)·CH_2Cl_2, and

Table 7. Atomic positional parameters (fractional co-ordinates) for (4)•CH_2Cl_2, with estimated standard deviations in parentheses

	Molecule A				Molecule B		
Atom	*x*	*y*	*z*	Atom	*x*	*y*	*z*
Ru(1)	0.719 5(2)	0.366	0.840 2(1)	Ru(1′)	0.681 8(2)	0.823 19(7)	0.802 2(1)
Ru(2)	0.661 4(2)	0.462 09(7)	0.800 0(1)	Ru(2′)	0.722 8(1)	0.725 54(7)	0.849 9(1)
Ru(3)	0.863 4(2)	0.422 01(8)	0.764 0(1)	Ru(3′)	0.522 4(1)	0.774 62(8)	0.871 6(1)
Ru(4)	0.641 8(1)	0.393 74(7)	0.638 8(1)	Ru(4′)	0.740 9(1)	0.797 88(7)	1.005 8(1)
Cu(1)	0.733 6(2)	0.400 5(1)	0.629 1(2)	Cu(1′)	0.632 7(2)	0.712 2(1)	1.012 5(2)
Cu(2)	0.533 6(2)	0.476 7(1)	0.617 7(2)	Cu(2′)	0.835 0(2)	0.713 5(1)	1.039 9(2)
P(1)	0.742 2(5)	0.537 3(2)	0.515 5(4)	P(1′)	0.619 4(5)	0.656 2(5)	1.121 8(4)
P(2)	0.444 3(4)	0.538 7(2)	0.532 2(4)	P(2′)	0.923 3(5)	0.653 4(2)	1.127 2(4)
O(1)	0.516(1)	0.320 1(7)	0.862(1)	O(1′)	0.909(1)	0.060 7(8)	0.003(1)
O(2)	0.819(2)	0.369 9(9)	1.067(1)	O(2′)	0.597(2)	0.815 2(7)	0.574(1)
O(3)	0.815(2)	0.272 2(9)	0.833(2)	O(3′)	0.586(1)	0.925 3(7)	0.796(1)
O(4)	0.751(2)	0.488 6(9)	1.019(1)	O(4′)	0.639(2)	0.697 3(8)	0.628(1)
O(5)	0.445(1)	0.149 9(9)	0.826(2)	O(5′)	0.954(1)	0.747 9(7)	0.837(1)
O(6)	0.601(1)	0.571 1(6)	0.759(1)	O(6′)	0.775(1)	0.620 2(6)	0.895(1)
O(7)	0.981(1)	0.429 1(8)	0.984(1)	O(7′)	0.411(2)	0.765 3(9)	0.650(1)
O(8)	1.030(1)	0.485 4(7)	0.700(1)	O(8′)	0.341(1)	0.725 4(8)	0.941(1)
O(9)	0.978(1)	0.330 1(6)	0.735(1)	O(9′)	0.420(1)	0.869 1(9)	0.888(2)
O(10)	0.424(1)	0.356 0(8)	0.647(1)	O(10′)	0.980(1)	0.817 0(7)	1.019(1)
O(11)	0.711(2)	0.292 6(6)	0.587(1)	O(11′)	0.711(2)	0.906 3(7)	1.032(1)
O(12)	0.566(2)	0.410 2(8)	0.417(1)	O(12′)	0.781(2)	0.780 9(8)	1.234(1)
C(1)	0.589(2)	0.356 3(8)	0.854(1)	C(1′)	0.824(2)	0.843 0(8)	0.801(1)
C(2)	0.788(2)	0.366(1)	0.980(2)	C(2′)	0.627(2)	0.817 5(8)	0.661(1)
C(3)	0.779(2)	0.311(1)	0.832(2)	C(3′)	0.624(2)	0.887 7(9)	0.802(2)
C(4)	0.723(2)	0.477(1)	0.935(1)	C(4′)	0.667(2)	0.718 3(8)	0.709(2)
C(5)	0.528(2)	0.442(1)	0.814(2)	C(5′)	0.863(2)	0.742 5(9)	0.844(1)
C(6)	0.623(2)	0.531 2(9)	0.767(1)	C(6′)	0.758(2)	0.658 0(8)	0.888(1)
C(7)	0.938(2)	0.424(1)	0.903(2)	C(7′)	0.457(2)	0.773(1)	0.735(2)
C(8)	0.962(2)	0.464(1)	0.714(2)	C(8′)	0.413(2)	0.741 8(9)	0.917(2)
C(9)	0.935(2)	0.364(1)	0.745(2)	C(9′)	0.466(2)	0.834(2)	0.883(2)
C(10)	0.509(2)	0.375 1(9)	0.646(2)	C(10′)	0.889(2)	0.813 0(9)	1.008(2)
C(11)	0.691(2)	0.331(1)	0.610(2)	C(11′)	0.717(3)	0.865 8(8)	1.013(2)
C(12)	0.592(2)	0.413 3(9)	0.503(1)	C(12′)	0.769(2)	0.784 7(9)	1.149(2)
C(13)	0.616(2)	0.562 2(8)	0.443(2)	C(13′)	0.749(2)	0.632 7(9)	1.204(1)
C(14)	0.536(2)	0.582 5(9)	0.500(1)	C(14′)	0.827(2)	0.609 5(8)	1.149(2)
C(15)	0.812(2)	0.514 7(8)	0.421(1)	C(15′)	0.544(2)	0.673 1(8)	1.214(1)
C(16)	0.758(2)	0.492(1)	0.336(2)	C(16′)	0.433(2)	0.667(1)	1.196(2)
C(17)	0.904(2)	0.479(1)	0.280(2)	C(17′)	0.385(2)	0.683(1)	1.267(2)
C(18)	0.800(2)	0.473(1)	0.269(2)	C(18′)	0.440(2)	0.707(1)	1.354(2)
C(19)	0.978(2)	0.500(1)	0.365(2)	C(19′)	0.542(2)	0.712(1)	1.368(2)
C(20)	0.013(2)	0.522(1)	0.428(2)	C(20′)	0.600(2)	0.699(1)	1.303(2)
C(21)	0.016(2)	0.590 1(9)	0.563(1)	C(21′)	0.546(2)	0.603 0(8)	1.066(1)
C(22)	0.839(2)	0.629 1(9)	0.504(2)	C(22′)	0.500(2)	0.599 6(9)	0.961(2)
C(23)	0.892(2)	0.665(1)	0.554(2)	C(23′)	0.440(2)	0.558 9(8)	0.920(2)
C(24)	0.936(2)	0.672 6(9)	0.643(2)	C(24′)	0.428(2)	0.521 8(8)	0.981(2)
C(25)	0.920(2)	0.635(1)	0.705(3)	C(25′)	0.463(2)	0.526(1)	1.079(2)
C(26)	0.862(2)	0.596 6(8)	0.667(2)	C(26′)	0.528(3)	0.565(1)	1.122(2)
C(27)	0.364(2)	0.573 3(9)	0.598(1)	C(27′)	1.010(2)	0.665 5(9)	1.253(2)
C(28)	0.275(2)	0.550 7(9)	0.619(2)	C(28′)	1.064(2)	0.628(1)	1.310(2)
C(29)	0.208(2)	0.577(1)	0.671(2)	C(29′)	1.133(2)	0.641(1)	1.409(2)
C(30)	0.230(2)	0.617 7(8)	0.706(2)	C(30′)	1.144(2)	0.685(1)	1.422(2)
C(31)	0.319(2)	0.642(1)	0.685(2)	C(31′)	1.082(2)	0.721(1)	1.306(2)
C(32)	0.387(2)	0.618 6(8)	0.633(1)	C(32′)	1.019(2)	0.710 6(9)	1.290(2)
C(33)	0.352(2)	0.525 4(8)	0.409(1)	C(33′)	1.012(2)	0.621 3(8)	1.061(1)
C(34)	0.326(2)	0.555(1)	0.329(2)	C(34′)	1.087(2)	0.650 5(8)	1.036(2)
C(35)	0.250(2)	0.539(1)	0.243(2)	C(35′)	1.156(2)	0.630(1)	0.987(2)
C(36)	0.199(2)	0.496(1)	0.231(2)	C(36′)	1.146(2)	0.580(1)	0.958(2)
C(37)	0.222(2)	0.465(1)	0.308(2)	C(37′)	1.064(2)	0.554 7(9)	0.977(2)
C(38)	0.296(2)	0.479 7(9)	0.404(2)	C(38′)	1.002(2)	0.573 2(9)	1.030(2)

Table 8. Atomic positional parameters (fractional co-ordinates) for (**5**)·CH_2Cl_2, with estimated standard deviations in parentheses

Atom	*x*	*y*	*z*	Atom	*x*	*y*	*z*
Ru(1)	0.883 88(8)	0.234 62(7)	0.823 15(5)	C(11)	0.862(1)	0.083 3(8)	0.723 4(6)
Ru(2)	0.777 64(8)	0.345 98(6)	0.742 41(5)	C(12)	0.734(1)	0.147 4(7)	0.620 6(7)
Ru(3)	0.967 96(8)	0.284 80(7)	0.725 42(5)	C(13)	0.639(1)	0.321 7(8)	0.500 3(6)
Ru(4)	0.793 72(8)	0.180 84(6)	0.705 18(5)	C(13A)	0.579(1)	0.385 2(8)	0.525 3(6)
Cu(1)	0.811 4(1)	0.302 5(1)	0.628 51(7)	C(14)	0.482(1)	0.359 3(9)	0.537 9(6)
Cu(2)	0.645 6(1)	0.274 2(1)	0.656 33(7)	C(15)	0.822(1)	0.272 6(9)	0.474 9(6)
P(1)	0.769 7(3)	0.332 3(2)	0.528 5(2)	C(16)	0.914(1)	0.296(1)	0.461 8(8)
P(2)	0.493 7(2)	0.286 0(2)	0.602 2(2)	C(17)	0.953(1)	0.250(1)	0.422 3(9)
O(1)	0.727 9(8)	0.207 0(9)	0.895 7(5)	C(18)	0.908(1)	0.180(1)	0.396 9(9)
O(2)	1.004 5(8)	0.337 6(6)	0.925 7(5)	C(19)	0.822(1)	0.160(1)	0.408 9(8)
O(3)	0.995(1)	0.083 8(6)	0.871 5(5)	C(20)	0.775(1)	0.204(1)	0.447 0(7)
O(4)	0.858(1)	0.466 4(7)	0.843 9(5)	C(21)	0.797(1)	0.434 0(8)	0.510 2(6)
O(5)	0.600 6(9)	0.319 1(8)	0.798 6(6)	C(22)	0.851(1)	0.481 7(9)	0.555 8(7)
O(6)	0.692 3(8)	0.485 9(6)	0.660 2(5)	C(23)	0.873(1)	0.559(1)	0.544 8(8)
O(7)	1.090 5(9)	0.402 0(8)	0.813 9(6)	C(24)	0.840(1)	0.592(1)	0.488 5(9)
O(8)	1.861 2(9)	0.328(1)	0.615 1(6)	C(25)	0.784(1)	0.546(1)	0.441 1(8)
O(9)	1.109 2(9)	0.153 3(8)	0.774 1(8)	C(26)	0.764(1)	0.466(1)	0.451 1(7)
O(10)	0.632 5(8)	0.125 3(8)	0.766 5(5)	C(27)	0.416 4(9)	0.325 2(8)	0.652 2(6)
O(11)	0.902 6(8)	0.025 0(6)	0.730 5(5)	C(28)	0.342(1)	0.283 3(8)	0.668 9(7)
O(12)	0.705 5(8)	0.121 9(6)	0.573 2(5)	C(29)	0.290(1)	0.313(1)	0.708 7(8)
C(1)	0.782(1)	0.217(1)	0.867 3(7)	C(30)	0.309(1)	0.387(1)	0.734 6(7)
C(2)	0.957(1)	0.300 2(8)	0.886 6(7)	C(31)	0.381(1)	0.431(1)	0.718 1(8)
C(3)	0.953(1)	0.139 5(9)	0.851 4(7)	C(32)	0.436(1)	0.401 5(9)	0.676 8(7)
C(4)	0.834(1)	0.118 9(9)	0.808 2(7)	C(33)	0.431 9(9)	0.196 1(8)	0.567 9(6)
C(5)	0.669(1)	0.327 0(9)	0.776 1(7)	C(34)	0.472(1)	0.122 9(9)	0.585 3(8)
C(6)	0.721(1)	0.430 4(8)	0.686 9(6)	C(35)	0.427(1)	0.054(1)	0.559 5(9)
C(7)	1.043(1)	0.358(1)	0.782 5(7)	C(36)	0.344(1)	0.056(1)	0.517 4(9)
C(8)	1.018(1)	0.311(1)	0.655 8(8)	C(37)	0.300(1)	0.130(1)	0.499 7(9)
C(9)	1.055(1)	0.201(1)	0.755 8(8)	C(38)	0.344(1)	0.199 6(9)	0.527 1(8)
C(10)	0.696(1)	0.148 7(9)	0.742 5(7)				

Table 9. Atomic positional parameters (fractional co-ordinates) for (**7**)·CH_2Cl_2, with estimated standard deviations in parentheses

Atom	*x*	*y*	*z*	Atom	*x*	*y*	*z*
Ru(1)	1.206 39(6)	0.298 81(4)	−0.252 39(5)	C(11)	0.982 0(8)	0.238 9(5)	−0.217 8(6)
Ru(2)	1.031 78(6)	0.290 75(3)	−0.403 84(5)	C(12)	0.814 8(8)	0.319 3(4)	−0.242 2(6)
Ru(3)	1.095 21(7)	0.389 82(3)	−0.317 78(5)	C(13)	0.565 7(8)	0.369 2(4)	−0.426 2(7)
Ru(4)	0.974 49(6)	0.308 45(3)	−0.244 21(5)	C(13A)	0.507 7(8)	0.352 5(4)	−0.483 4(7)
Cu(1)	0.863 36(9)	0.360 66(5)	−0.382 68(8)	C(13B)	0.579 1(8)	0.304 5(4)	−0.474 0(6)
Cu(2)	0.837 4(1)	0.259 69(5)	−0.372 06(8)	C(13C)	0.518 9(9)	0.258 3(5)	−0.518 5(7)
Cl(1)	0.471 9(6)	0.586 0(3)	0.177 8(4)	C(14)	0.601 1(8)	0.214 1(4)	−0.523 1(6)
Cl(2)	0.432 3(8)	0.490 4(3)	0.090 9(5)	C(15)	0.737 8(8)	0.475 2(4)	−0.373 3(7)
P(1)	0.713 6(2)	0.414 0(1)	−0.432 9(2)	C(16)	0.737(1)	0.522 0(4)	−0.409 9(7)
P(2)	0.704 5(2)	0.199 1(1)	−0.420 3(2)	C(17)	0.762(1)	0.565 4(5)	−0.360 9(8)
O(1)	1.249 7(6)	0.191 2(3)	−0.184 3(5)	C(18)	0.787(1)	0.562 1(5)	−0.276(1)
O(2)	1.423 1(6)	0.295 6(4)	−0.318 3(6)	C(19)	0.787(1)	0.515 7(6)	−0.236 9(8)
O(3)	1.333 7(7)	0.343 7(4)	−0.084 7(6)	C(20)	0.763(1)	0.472 3(5)	−0.287 5(8)
O(4)	1.079 0(7)	0.177 5(3)	−0.368 8(5)	C(21)	0.692 6(8)	0.433 1(4)	−0.541 3(6)
O(5)	0.842 6(6)	0.275 3(4)	−0.567 8(4)	C(22)	0.782(1)	0.423 6(5)	−0.579 0(7)
O(6)	1.214 3(6)	0.292 2(4)	−0.502 8(5)	C(23)	0.772(1)	0.438 8(5)	−0.661 7(8)
O(7)	1.305 9(6)	0.403 6(4)	−0.385 8(6)	C(24)	0.673(1)	0.461 7(6)	−0.707 8(7)
O(8)	0.994 7(7)	0.490 7(3)	−0.402 7(6)	C(25)	0.583(1)	0.471 9(5)	−0.671 5(8)
O(9)	1.208 6(9)	0.443 7(4)	−0.154 9(6)	C(26)	0.593(1)	0.475 5(5)	−0.588 2(7)
O(10)	1.080 6(8)	0.335 4(5)	−0.059 8(5)	C(27)	0.775 9(9)	0.140 3(4)	−0.438 5(7)
O(11)	0.982 8(6)	0.195 7(3)	−0.199 4(5)	C(28)	0.806(1)	0.130 9(6)	−0.512 8(8)
O(12)	0.726 3(6)	0.324 5(4)	−0.227 9(5)	C(29)	0.866(1)	0.087 1(6)	−0.521 9(9)
C(1)	1.230 8(8)	0.233 2(4)	−0.211 4(7)	C(30)	0.897(1)	0.052 5(6)	−0.459(1)
C(2)	1.342 2(9)	0.297 8(5)	−0.295 5(7)	C(31)	0.879(2)	0.063 0(7)	−0.382(1)
C(3)	1.284 1(9)	0.327 1(4)	−0.149 6(7)	C(32)	0.814(1)	0.106 3(5)	−0.373 6(9)
C(4)	1.062 7(8)	0.221 6(4)	−0.378 8(7)	C(33)	0.613 0(8)	0.180 4(4)	−0.351 9(6)
C(5)	0.906 8(8)	0.283 0(5)	−0.504 0(6)	C(34)	0.647 5(9)	0.191 7(5)	−0.267 7(7)
C(6)	1.149 2(9)	0.292 5(5)	−0.463 9(7)	C(35)	0.582(1)	0.176 4(5)	−0.214 3(7)
C(7)	1.229 1(8)	0.396 6(5)	−0.359 3(8)	C(36)	0.478 7(9)	0.151 5(5)	−0.245 3(8)
C(8)	1.023 3(8)	0.451 1(5)	−0.372 3(7)	C(37)	0.441 8(9)	0.139 4(6)	−0.329 2(8)
C(9)	1.167(1)	0.421 3(5)	−0.216 1(8)	C(38)	0.508(1)	0.154 0(5)	−0.382 8(7)
C(10)	1.043(1)	0.325 9(5)	−0.130 8(7)	C(39)	0.464(2)	0.552 1(7)	0.085(1)

(**7**)·CH_2Cl_2, respectively. Additional material available from the Cambridge Crystallographic Data Centre comprises thermal parameters, H-atom co-ordinates, and remaining bond parameters.

Acknowledgements

We thank Professor W. McFarlane for helpful discussions, Dr. V. Šik for the ^1H n.m.r. simulations, and Drs. O. W. Howarth and E. H. Curzon for recording a number of 400-MHz ^1H n.m.r. spectra. In addition, we thank the S.E.R.C. for a studentship (to S. S. D. B.), the Nuffield Foundation for support, Johnson Matthey Ltd. for a generous loan of silver and ruthenium salts, Mr. R. J. Lovell for technical assistance, and Mrs. L. J. Salter for drawing the diagrams.

References

1 Part 5, T. Adatia, M. McPartlin, and I. D. Salter, preceding paper.

2 I. D. Salter, Adv. Dynamic Stereochem., 1987, vol. 2, in the press and refs. therein.

3 M. J. Freeman, A. G. Orpen, and I. D. Salter, *J. Chem. Soc., Dalton Trans.*, 1987, 379.

4 For example, M. J. Freeman, A. G. Orpen, and I. D. Salter, *J. Chem. Soc., Dalton Trans.*, 1987, 1001 and refs. therein.

5 S. S. D. Brown, S. Hudson, I. D. Salter, and M. McPartlin, *J. Chem. Soc., Dalton Trans.*, 1987, 1967.

6 P. A. Bates, S. S. D. Brown, A. J. Dent, M. B. Hursthouse, G. F. M. Kitchen, A. G. Orpen, I. D. Salter, and V. Šik, *J. Chem. Soc., Chem. Commun.*, 1986, 600.

7 S. S. D. Brown, P. J. McCarthy, and I. D. Salter, *J. Organomet. Chem.*, 1986, **306**, C27.

8 J. A. K. Howard, I. D. Salter, and F. G. A. Stone, *Polyhedron*, 1984, **3**, 567.

9 C. E. Briant, K. P. Hall, and D. M. P. Mingos, *J. Chem. Soc., Chem. Commun.*, 1983, 843.

10 S. R. Bunkhall, H. D. Holden, B. F. G. Johnson, J. Lewis, G. N. Pain, P. R. Raithby, and M. J. Taylor, *J. Chem. Soc., Chem. Commun.*, 1984, 25.

11 S. S. D. Brown, I. D. Salter, and B. M. Smith, *J. Chem. Soc., Chem. Commun.*, 1985, 1439.

12 R. A. Brice, S. C. Pearse, I. D. Salter, and K. Henrick, *J. Chem. Soc., Dalton Trans.*, 1986, 2181.

13 J. S. Bradley, R. L. Pruett, E. Hill, G. B. Ansell, M. E. Leonowicz, and M. A. Modrick, *Organometallics*, 1982, **1**, 748.

14 B. F. G. Johnson, J. Lewis, W. J. H. Nelson, M. D. Vargas, D. Braga, K. Henrick, and M. McPartlin, *J. Chem. Soc., Dalton Trans.*, 1986, 975.

15 G. V. Goeden and K. G. Caulton, *J. Am. Chem. Soc.*, 1981, **103**, 7354.

16 S. S. D. Brown, I. D. Salter, V. Šik, I. J. Colquhoun, W. McFarlane, P. A. Bates, M. B. Hursthouse, and M. Murray, *J. Chem. Soc., Dalton Trans.*, in the press.

17 S. S. D. Brown and I. D. Salter, *Organomet. Synth.*, 1988, **4**, in the press.

18 G. J. Kubas, *Inorg. Synth.*, 1979, **19**, 90.

19 S. S. D. Brown and I. D. Salter, *Organomet. Synth.*, 1986, **3**, 315.

Received 22nd April 1987; *Paper* 7/725